SUPPLEMENTARY INFORMATION

Fiber Emission of Carbon Nanotube Containing Materials for Construction Applications

Candace S.J. Tsai[1,2,3]*, Nara Shin[2], Anthony Formella[3]

[1]Department of Environmental Health Sciences, Field School of Public Health, University of California, Los Angeles, Los Angeles, CA 90095

[2]Department of Environmental and Radiological Health Sciences, Colorado State University, Fort Collins, CO 80523

[3]Department of Chemical and Biological Engineering, Colorado State University, Fort Collins, CO 80523

*Corresponding author: Dr. Candace S.J. Tsai

Department of Environmental Health Sciences, Field School of Public Health, University of California, Los Angeles, Los Angeles, CA 90095

Address: 650 Charles E. Young Drive S., MC 177220, Los Angeles, California 90095

Email: candacetsai@ucla.edu

Phone: +1 (310) 206-5296

TABLE OF CONTENT

Figure S7. SEM and EDS analysis results of the image from product B by TDS. (a) Area selected for analysis. (b) Peaks analyzed by EDS. (c) Colorimetric elemental intensity analysis via EDS of a particle in image (a).

Figure S8. SEM and EDS analysis results of the image from product C by TDS. (a) Area selected for analysis. (b) Peaks analyzed by EDS. (c) Colorimetric elemental intensity analysis via EDS of a particle in image (a).

Figure S9. SEM and EDS analysis results of the image from product D by TDS. (a) Area selected for analysis. (b) Peaks analyzed by EDS. (c) Colorimetric elemental intensity analysis via EDS of a particle in image (a).

Figure S10. TEM and EDS analysis of particles collected from product A on a TEM grid by TDS. (a) The area of particles with small particulates attached to the edge,(b) Element peaks observed from analyzing the area in (a). (c) Colorimetric elemental intensity analysis via EDS for the area in (a).

Figure S11. TEM and EDS analysis of particles collected from product B on a TEM grid by TDS. (a) The particle selected for EDS analysis, (b) Element peaks observed from analyzing the area in (a). (c) Colorimetric elemental intensity analysis via EDS for the area in (a).

Figure S12. TEM and EDS analysis of the particles collected from product C on a TEM grid by TDS. (a) The area selected for analysis. (b) Element peaks analyzed by EDS. (c) Colorimetric elemental intensity analysis via EDS of image (a).

Figure S13. TEM and EDS analysis of the particles collected from product D on a TEM grid by TDS. (a) The area selected for analysis. (b) Element peaks analyzed by EDS. (c) Colorimetric elemental intensity analysis via EDS of image (a).

Figure S14. Particle size-fractioned concentrations in average with original concentration data during brushing shown in tan color dots. Concentrations in size range of 10-420 nm measured by NanoScan SMPS were shown on the left column. Concentrations in size range of 0.3-10 μm measured by OPS were shown on the right column. Concentrations were presented with measurements prior the test, during the testing activity (brushing or grinding), during idle period, and post the test. (a) and (b) Tests for brushing CNT coated tile, sample code A, (c) and (d) Tests for brushing non-CNT coated tile, sample code B, (e) and (f) Tests for grinding CNT containing concrete, sample code C, (g) and (h) Tests for grinding non-CNT containing concrete, sample code D.

Dynamic Aerosol Behavior

Method of Preparing Concrete Tiles and Cylinders

To prepare the concrete tile product for simulating a dried spill, the concrete surfaces were prepared with commercially available paving tiles approximately 7 in × 7 in × 1.5 in. Painter's tape, 2 in wide, was wrapped around the outside edges, with about 1 in of tape stuck to the tile and 1 in projecting above the top surface. A water-tight dam around the outside of the top tile surface was made by filling the inside corner between the tape and the top of the tile with a ~1/4 in diameter bead of silicone-based caulking material. After the caulking had cured, 100 ml of liquid admixture was poured onto the top of the tiles, inside the silicone dam, and the tiles were dried in an oven at 70 °C for 24 hours and sealed in plastic bags after cooling.

The concrete cylinders to be evaluated were made using 4 in diameter × 8 in long plastic cylinder molds. The typical concrete mix used a liquid admixture dose equivalent to 2 gallons per cubic yard of concrete, which replaced 2 gallons of the reference concrete mix water, where applicable. The cylinders were filled and cured according to American Society for Testing and Materials (ASTM) C192 standards (ASTM C192/C192M-19 2019). The liquid admixture containing CNTs and the reference admixture without CNTs for control samples were used.

Specific Methods of Sampling and Analysis

1) NMAM 7402

NMAM 7402 is a method using transmission electron microscopy (TEM) for fibers such as asbestos [40]. In this study, the sampling method for NMAM 7402 was modified according to studies by a NIOSH field team using a three-piece open-faced sampling cassette to collect CNTs and carbon nanofibers (CNFs) for qualitative fiber identification [34, 41]. The sampling cassettes (25-mm, three-piece open faced) were used to collect particles on a 0.45 μm porous mixed cellulose ester (MCE) filter with a support pad operating at a flow rate of 2.0 L/min. One cassette was used for each experiment. After particle collection, the cassettes were enclosed and sent to Bureau Veritas (Maxxam Analytics, A Bureau Veritas Group Company, Kennesaw, GA, USA) for preparation of transferring collected particles from the MCE filter onto the TEM grids. Each sampled MCE filter was prepared for three TEM grids and mailed back to authors, then analyzed at the university central facility through TEM (JOEL, JEM-2100F, JOEL, Peabody, MA, USA) and energy dispersive X-ray spectroscopy (EDS) (model 51-XMX1058, Concord, MA, USA) at 200 kV to determine the morphological characteristics and elemental compositions.

2) Sampling using TDS

The TDS is a sampling method designed for respirable and nanoparticle collection [42, 43]. It has features to efficiently collect particles in low concertation environments or for short term sampling when the particle mass often is below the limits of detection of other methods. The sampling substrates were a silicon oxide filmed TEM grid and a 25-mm diameter 0.22-μm pore size polycarbonate membrane filter (Millipore, Billerica, MA, USA) with the grid attached at the center of the filter, and TDS was operated at a flow rate of 0.3 L/min. One polycarbonate filter and one TEM grid were used to collect particles for each experiment. All cassettes were weighed before

and after the experiments to obtain the total mass concentrations and were kept sealed until the microscopic analysis. Particles collected on the filter and on the grid using TDS were analyzed separately. Particles collected on the polycarbonate filters were analyzed through scanning electron microscopy (SEM) (JSM-6500F, JOEL, Peabody, MA, USA) and attached EDS (model 51-XMX1015, Concord, MA, USA) at 15 kV to determine particle characteristics and elemental compositions. The grids were analyzed with TEM and EDS at 200 kV.

3) Airborne particle measurements

Direct RTIs including a NanoScan scanning mobility particle sizer (NanoScan SMPS) and an optical particle sizer (OPS) were used for concentration measurements in this study. These two instruments measure particle size ranges of 10–420 nm and 0.3–10 μm, respectively, and provide the size-fractionated particle number concentration with a 1 min response time.

4) NMAM 5040

NMAM 5040 is a method used to analyze elemental carbon (EC), which is recommended by NIOSH for CNT analysis. The current recommended exposure limit (REL) by NIOSH for CNTs is 1 $\mu g/m^3$ of EC. The sampler is a three-piece 25-mm open-faced cassette with a quartz filter operating at a flow rate of 2.0 L/min. One cassette was used for each experiment. All cassettes and samples were prepared and analyzed by Maxxam Analytics (Novi, MI, USA), through evolved gas analysis with a thermal-optical analyzer to obtain EC mass concentration.

5) NMAM 7500

NMAM 7500 is a method used as a part of the current regulatory requirements for evaluating crystalline silica exposure. In 2016, OSHA announced the enforcement of the new regulation of the permissible exposure limit for respirable crystalline silica, which was reduced from 250 $\mu g/m^3$ to 50 $\mu g/m^3$, averaged over an 8-hour day. The threshold limit value (TLV) recommended by

American Conference of Governmental Industrial Hygienists (ACGIH) is 0.1 mg/m^3 for quartz and is 0.05 mg/m^3 for cristobalite and tridymite. The sampler includes a three-piece 37-mm cassette, a 5 μm PVC membrane filter, and a 10-mm nylon cyclone operated at a 1.7 L/min flow rate for respirable particle collection. One cassette was used for each experiment. All cassettes and filter samples were prepared and sent to ALS Environmental (Salt Lake City, UT, USA) for concentration analysis through X-ray powder diffraction to obtain silica mass concentration.

Table S1: Number of particle images.

		Tile		Cylinder	
		A	**B**	**C**	**D**
NMAM 7402 TEM	Total number of images	21	8	17	24
	Number of images with CNT or fiber containing particles including multiple images of the same particle	6	0	0	0
	Number of singular images with CNT of fiber containing particles	1	0	0	0
TDS SEM	Total number of images	42	46	47	40
	Number of images with CNT or fiber containing particles including multiple images of the same particle	12	0	1	2
	Number of singular images with CNT of fiber containing particles	3	0	1	1
TDS TEM	Total number of images	57	56	63	60
	Number of images with CNT or fiber containing particles including multiple images of the same particle	22	1	17	2
	Number of singular images with CNT of fiber containing particles	6	1	4	1

Table S2: Statistical analysis results with comparisons of particle size distributions

		A_OPS	B_OPS	C_OPS	D_OPS			A_SMPS	B_SMPS	C_SMPS	D_SMPS
A_OPS	Pearson Correlation	1.000	.805**	-0.135	-0.466	A_SMPS	Pearson Correlation	1.000	.984**	0.036	0.268
	Sig.		0.000	0.618	0.069		Sig.		0.000	0.907	0.376
	N	16	16	16	16		N	13	13	13	13
B_OPS	Pearson Correlation	.805**	1.000	-0.429	-.638**	B_SMPS	Pearson Correlation	.984**	1.000	-0.008	0.184
	Sig.	0.000		0.098	0.008		Sig.	0.000		0.979	0.548
	N	16	16	16	16		N	13	13	13	13
C_OPS	Pearson Correlation	-0.135	-0.429	1.000	.932**	C_SMPS	Pearson Correlation	0.036	-0.008	1.000	.852**
	Sig.	0.618	0.098		0.000		Sig.	0.907	0.979		0.000
	N	16	16	16	16		N	13	13	13	13
D_OPS	Pearson Correlation	-0.466	-.638**	.932**	1.000	D_SMPS	Pearson Correlation	0.268	0.184	.852**	1.000
	Sig.	0.069	0.008	0.000			Sig.	0.376	0.548	0.000	
	N	16	16	16	16		N	13	13	13	13
**. Correlation is significant at the 0.01 level (2-tailed).						**. Correlation is significant at the 0.01 level (2-tailed).					

From Table S2, the analysis of emitted particles during brushing CNT containing A and non-CNT containing B tile products (Figures 5a-5d) resulted in a correlation coefficient of 0.984 for 10-420 nm size range and 0.805 for 0.3-10 µm sizes that indicated a high correlation. The correlation analysis between grinding CNT containing C and non-CNT containing D concrete cylinder products (Figures 5e-5h) showed a correlation coefficient of 0.852 for 10-420 nm size range and 0.932 for 0.3-10 µm sizes. In the comparison between brushing and grinding activities, the correlation between the brushing CNT containing tile A and grinding CNT containing

cylinder C showed the correlation coefficient of 0.036 for 10-420 nm sizes indicating very low correlation and -0.135 for 0.3-10 μm sizes indicating high difference; and the significance of p-values were 0.907 and 0.618 respectively meaning the correlations were not significantly different.

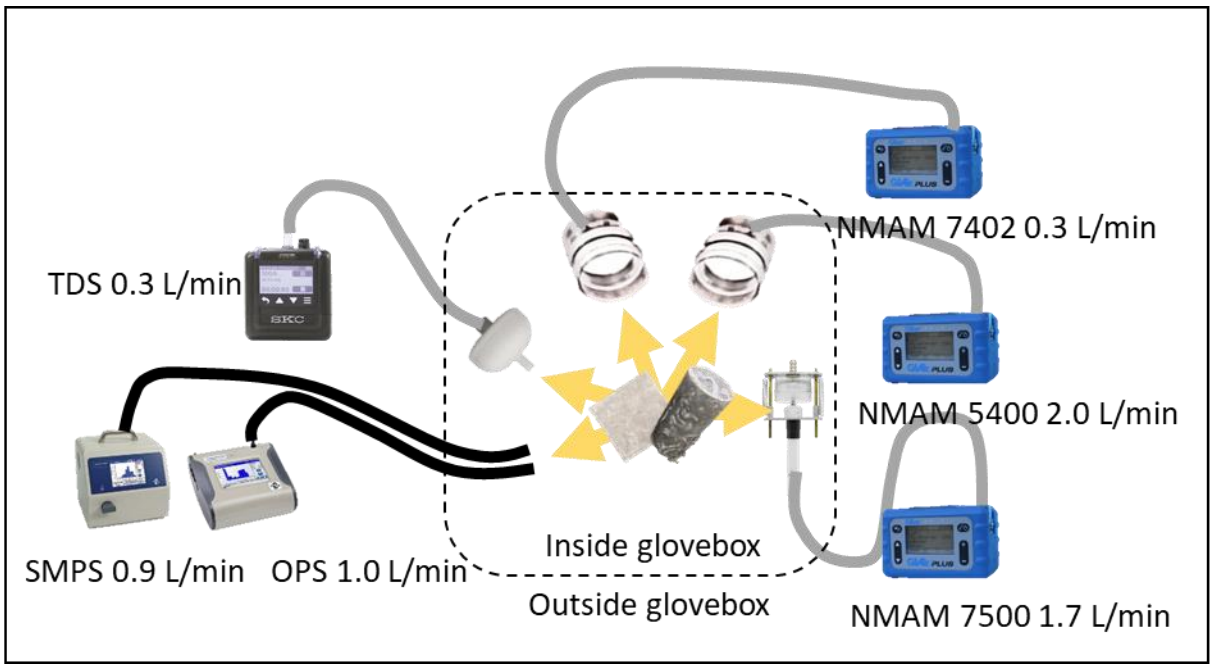

Figure S1. Experimental set up inside a glovebox.

The NanoScan SMPS was operated at a flow rate of 0.9 L/min, and the OPS was operated at a flow rate of 1.0 L/min. The statistical analysis was conducted using Pearson's correlation with the p-value of 0.01 via IBM SPSS statistics program (Version 21.0, IBM, Armonk, NY, USA). The size distribution data of airborne particles measured from RTIs were analyzed for correlation relationship between different types of product.

Elemental Composition Analysis Results

Airborne Substances Collected by NMAM 7402

The elemental composition analysis of particles from brushing CNT containing tile surface A, was shown in SI Figure S2; the analyzed particles, elemental compositions and colorimetric elemental intensities were presented respectively in a, b, and c of Figure S2. This order of presentation of EDS analysis result is consistent throughout all results presented in the SI figures. The particles were consisted of carbon (C), calcium (Ca), chromium (Cr), copper (Cu), iron (Fe), potassium (K), oxygen (O) and silicon (Si). Figure S3 showed the EDS results of particles released from brushing non-CNT containing tile surface B, with particles in round but relatively sharp-edged particles containing aluminum (Al), C, Ca, Cr, Cu, Fe, O, and Si. One distinctive difference between A and B products was the presence of element K in the CNT containing sample-A and Al in the non-CNT containing sample B. The EDS analysis result of particles released from grinding CNT containing concrete cylinder C were shown in Figure S4; released particles showed elements including Al, C, Ca, Cu, Fe, K, magnesium (Mg), sodium (Na), O and Si. The particles released during the grinding non-CNT containing concrete cylinder-D were presented in Figure S5; they contained similar elements as product C, with Cr as an addition.

Airborne Substances Collected by TDS

The full EDS analysis of product A was presented in Figure S6. Figure S7 shows the EDS results and SEM image of particles released from non-CNT containing tile product B. Common elements analyzed on particles from product A and B include Al, C, Ca, Cl, Cu, Mg, O, Si, and Zn, as graphed and mapped in Figures S6b, S7b, S6c and S7c. The only difference found between tile products A and B was the presence of Ca found in the particles released from non-CNT containing tile B. Figures S8 and S9 were SEM images and EDS analysis of particles collected

during grinding cylinder products C and D respectively. The common elements from grinding cylinder products were Al, C, Ca, Fe, K, Mg, Na, O and Si, whereas cylinder C contains Cl, Cu and Zn, and cylinder product D contains Titanium (Ti) additionally.

EDS with TEM analysis on particles collected on grids during brushing tile products A and B were listed in Figures S10 and S11 respectively. The elements found in the particles released from product A were Al, C, Ca, Cu, Fe, nickel (Ni), O, and Si. All these elements were also identified on particles released from tile product B, but Au, Cl, Cr, K, Na, S, and Ti were additional elements found. One representative particle agglomerate collected during grinding cylinder product C is presented with elemental compositions of EDS analysis as shown in Figure S12. Elements including Al, C, Cu, Chlorine (Cl), Fe, K, Mg, O, Si, and Ti were identified from the particles associated with CNT containing concrete cylinder. The non-CNT containing cylinder product D is analyzed and shown in Figure S13. Similar elements, Al, C, Ca, Fe, K, Mg, O, and Si, as seen in cylinder product C were also identified in cylinder product D but Na was found additionally in the released particles from cylinder product D.

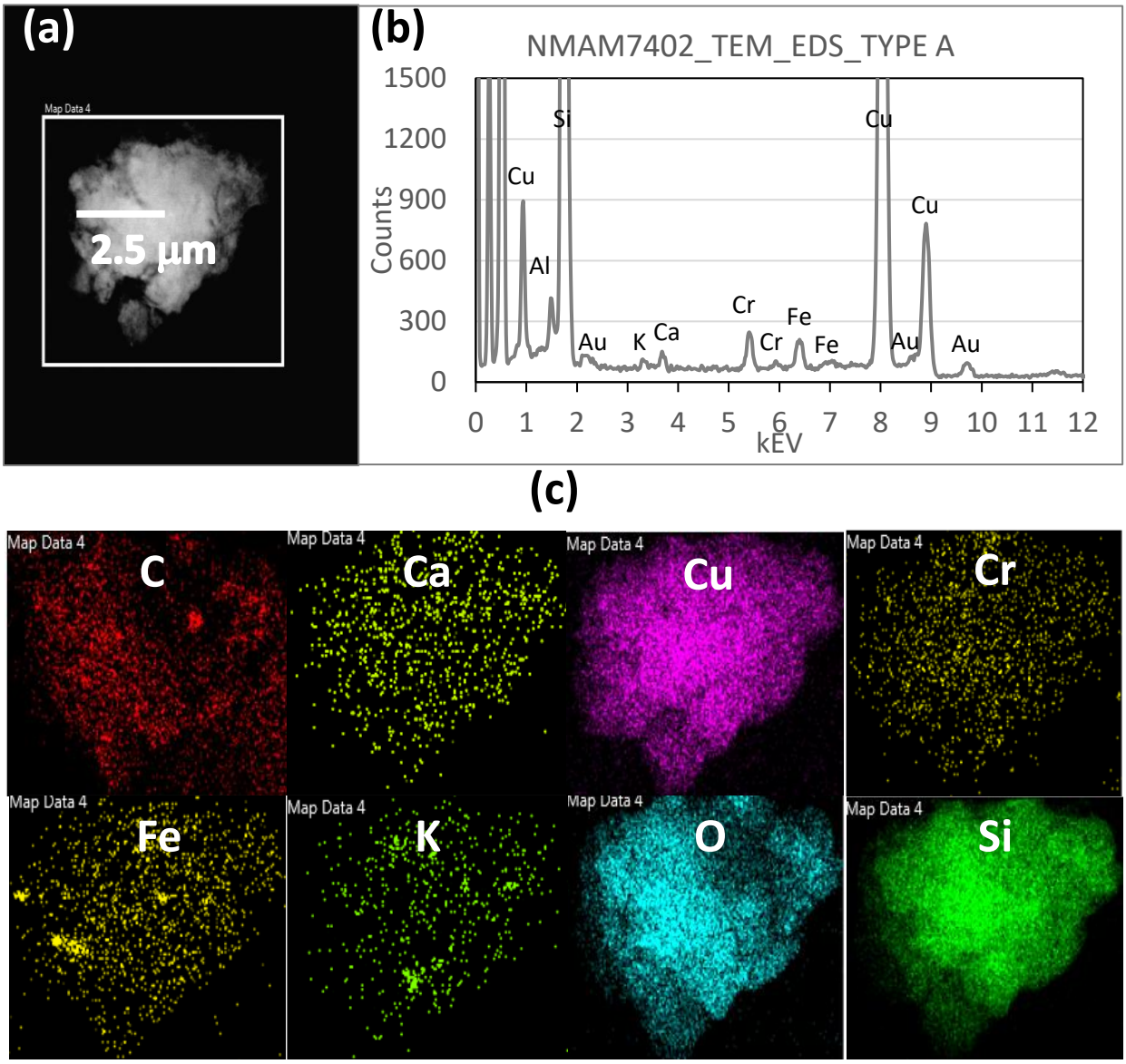

Figure S2. TEM and EDS analysis of a particle from product A using NMAM7402. (a) TEM image of a particle. (b) EDS analysis of the image in (a). (c) Colorimetric elemental intensity analysis via EDS of a particle in image (a).

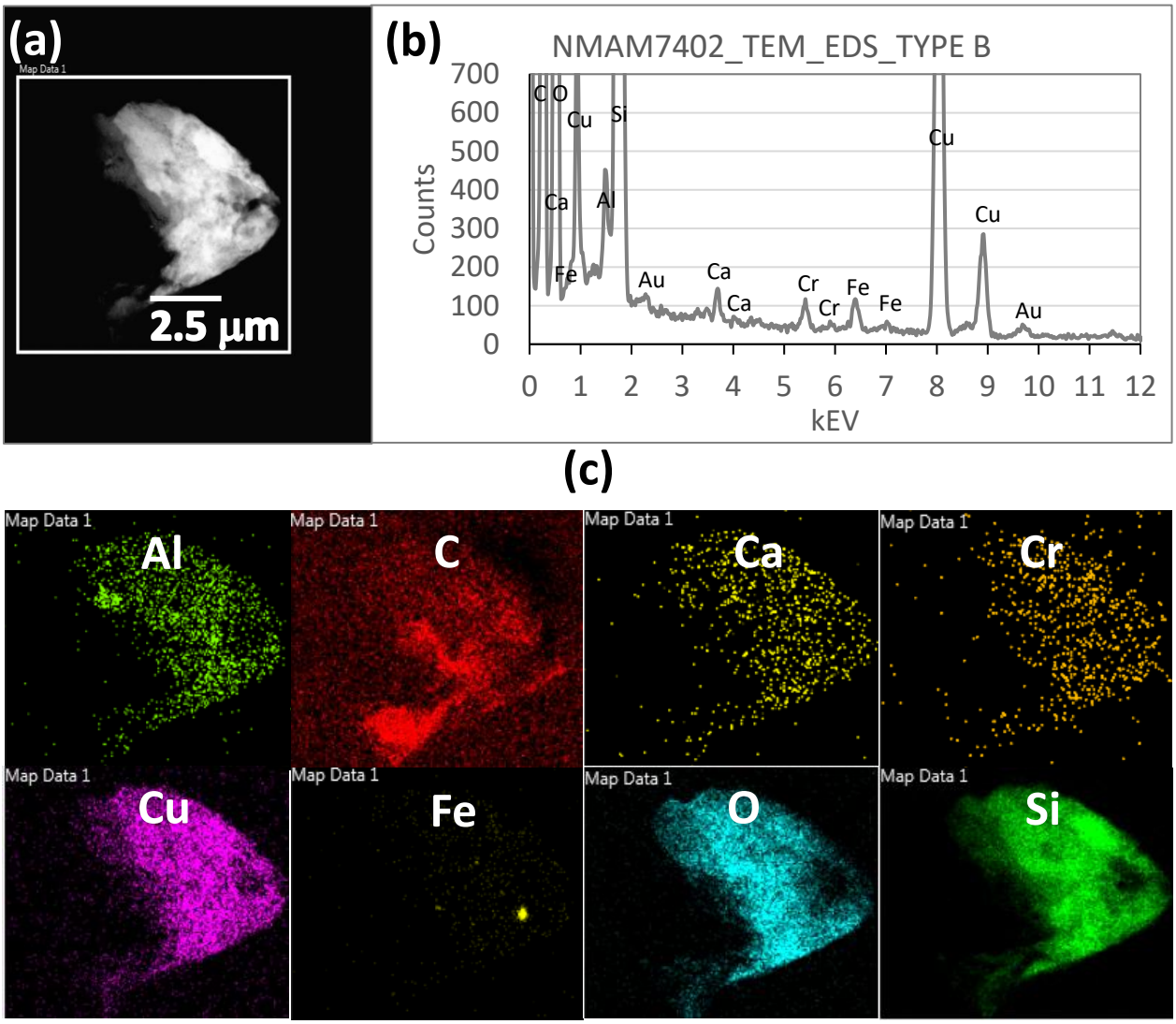

Figure S3. TEM and EDS analysis of a particle from product B using NMAM 7402. (a) TEM image of a particle. (b) EDS analysis of the image in (a). (c) Colorimetric elemental intensity analysis via EDS of a particle in image (a).

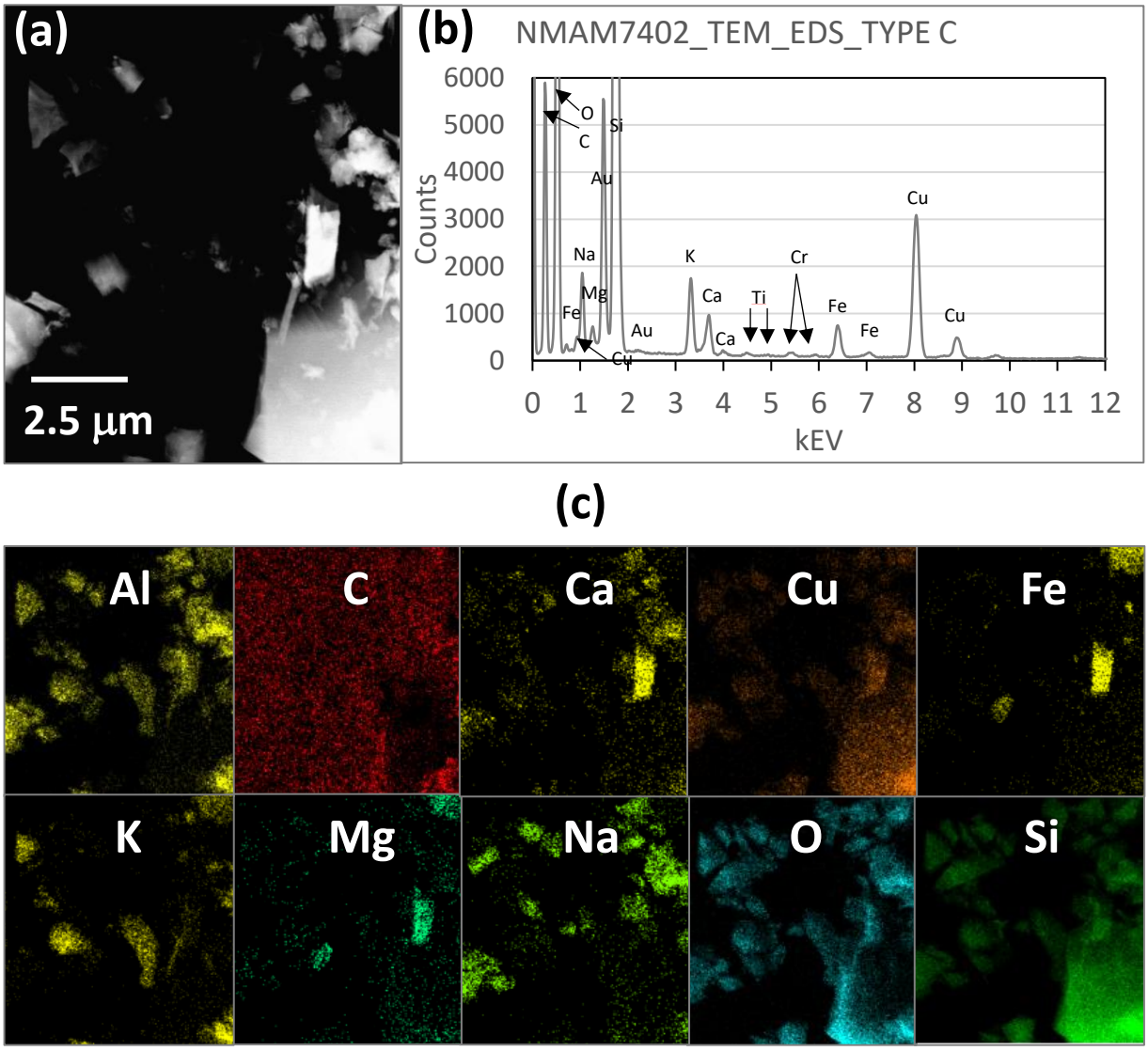

Figure S4. TEM and EDS analysis of particles from product C using NMAM 7402. (a) TEM image of particles. (b) EDS analysis of the image in (a). (c) Colorimetric elemental intensity analysis via EDS of particles in image (a).

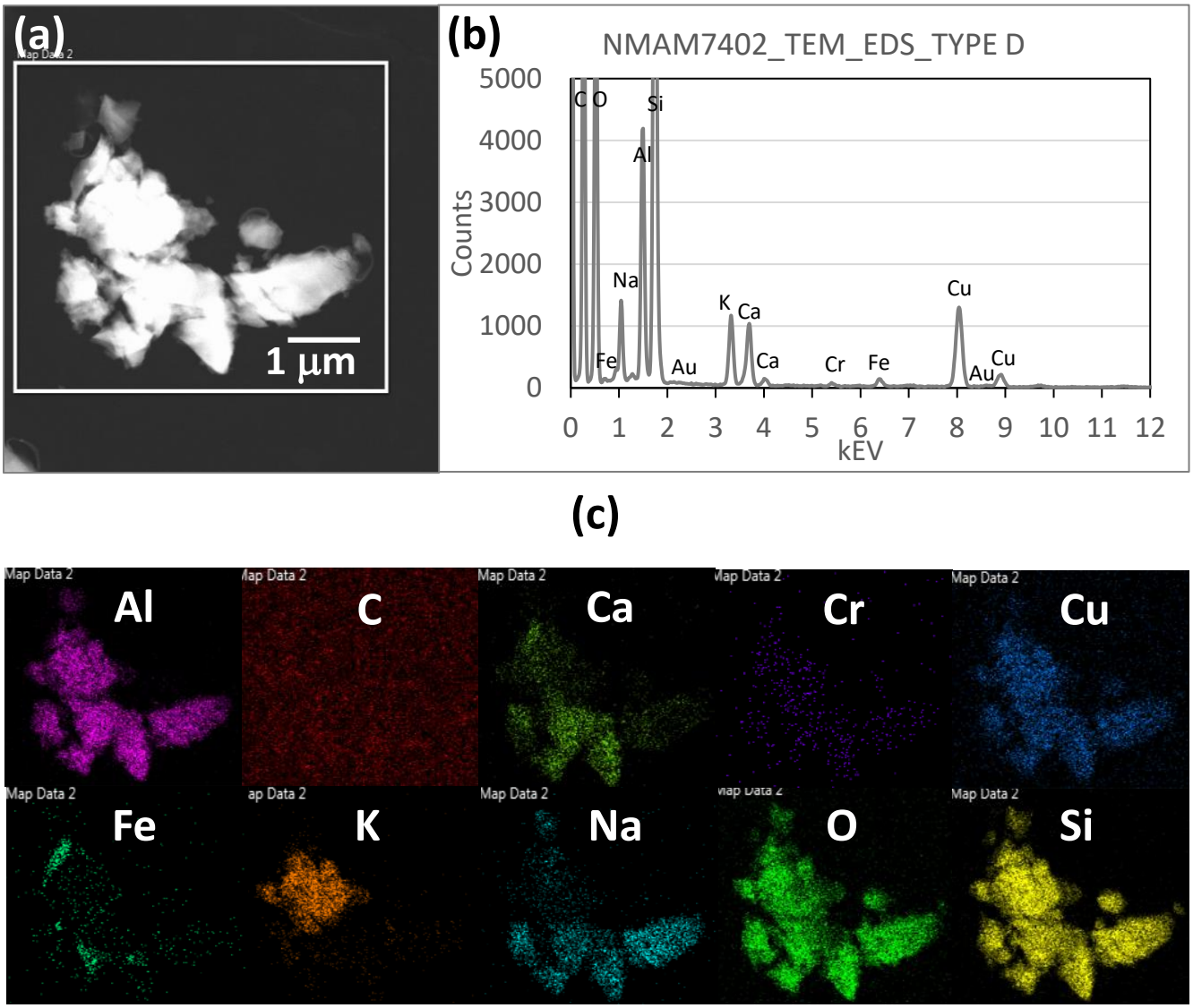

Figure S5. TEM and EDS analysis of particles from product D using NMAM 7402. (a) TEM image of particles. (b) EDS analysis of the image in (a). (c) Colorimetric elemental intensity analysis via EDS of particles in image (a).

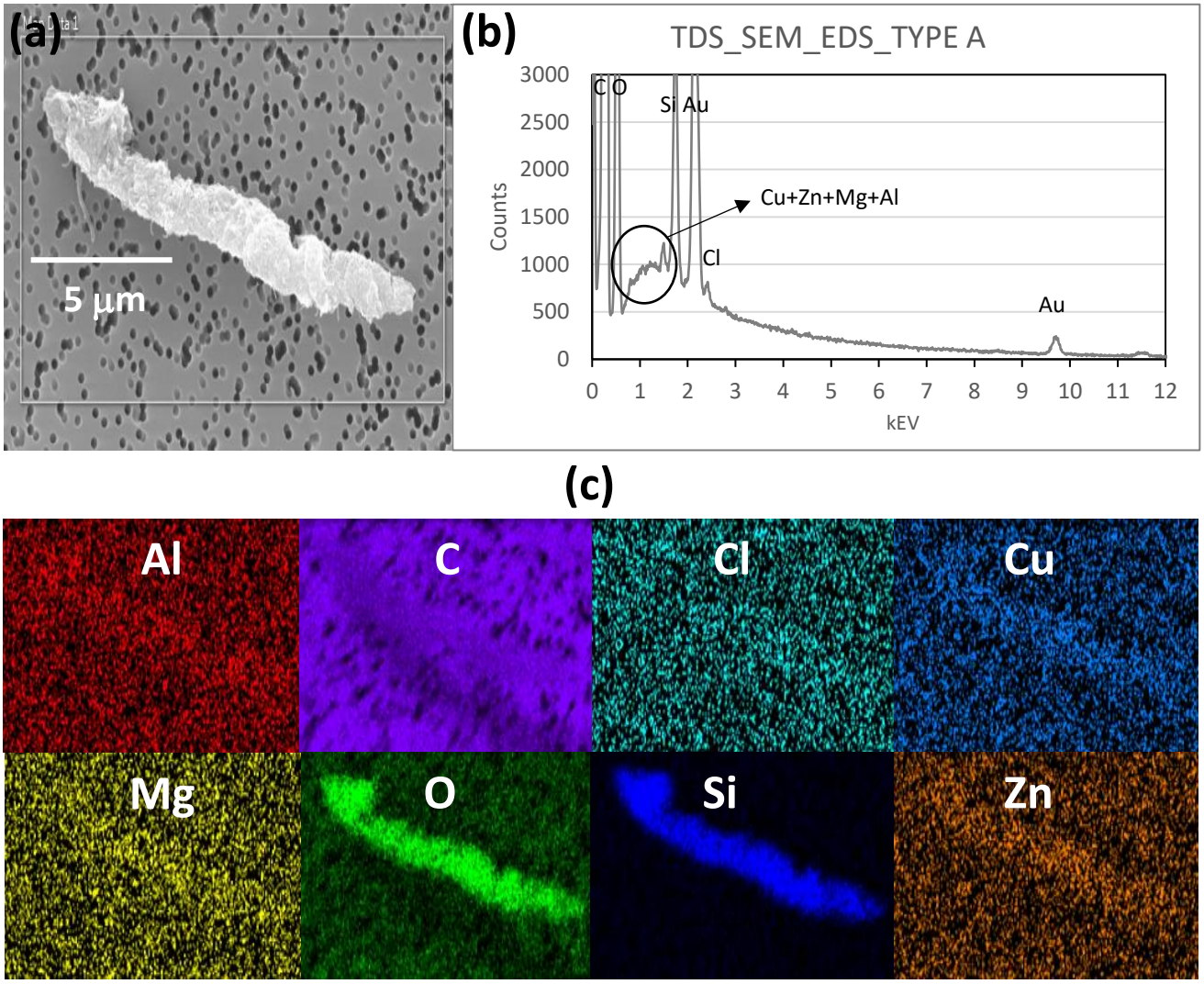

Figure S6. SEM and EDS analysis results of the image from product A by TDS. (a) Area selected for analysis. (b) Peaks analyzed by EDS. (c) Colorimetric elemental intensity analysis via EDS of a particle in image (a).

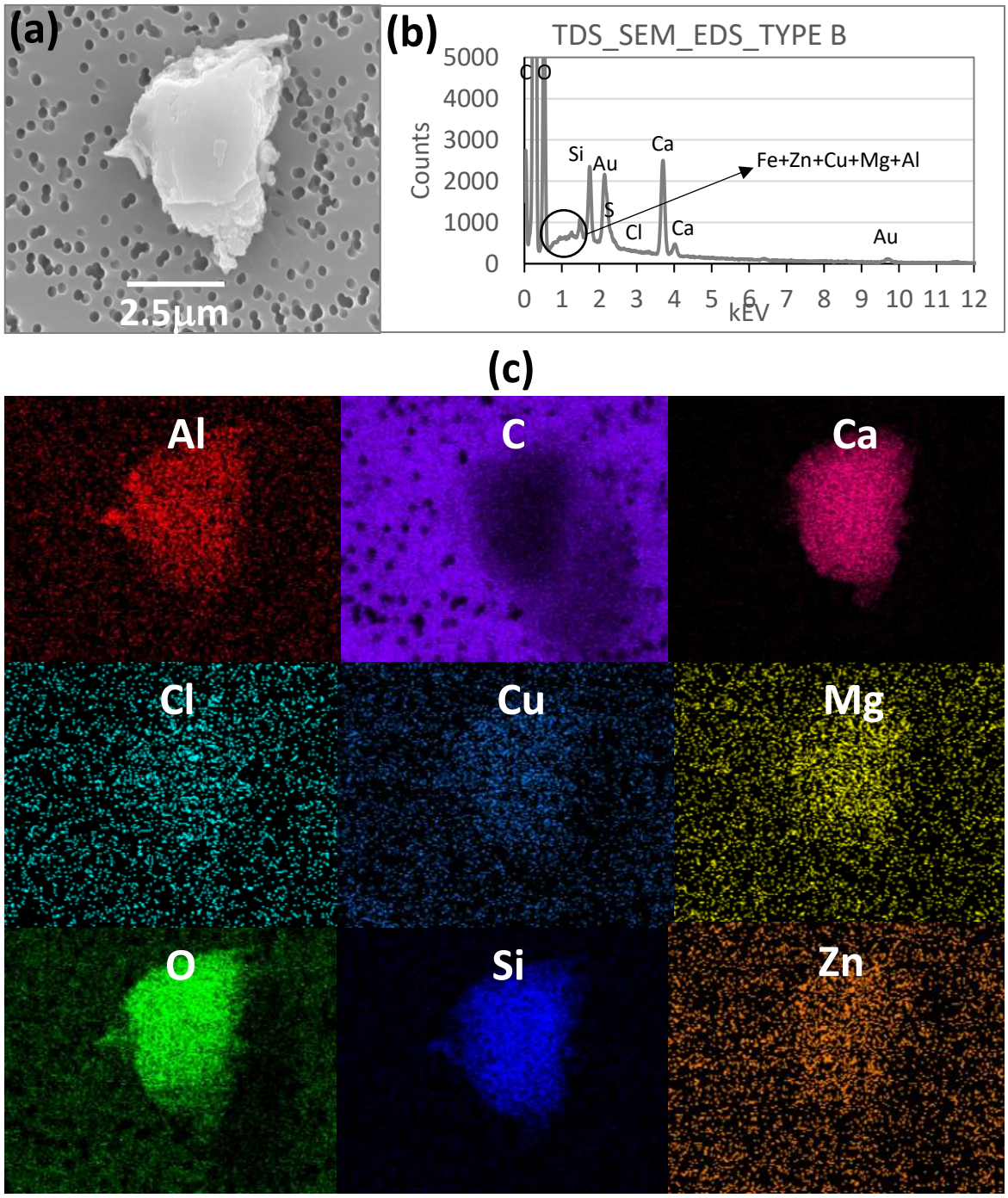

Figure S7. SEM and EDS analysis results of the image from product B by TDS. (a) Area selected for analysis. (b) Peaks analyzed by EDS. (c) Colorimetric elemental intensity analysis via EDS of a particle in image (a).

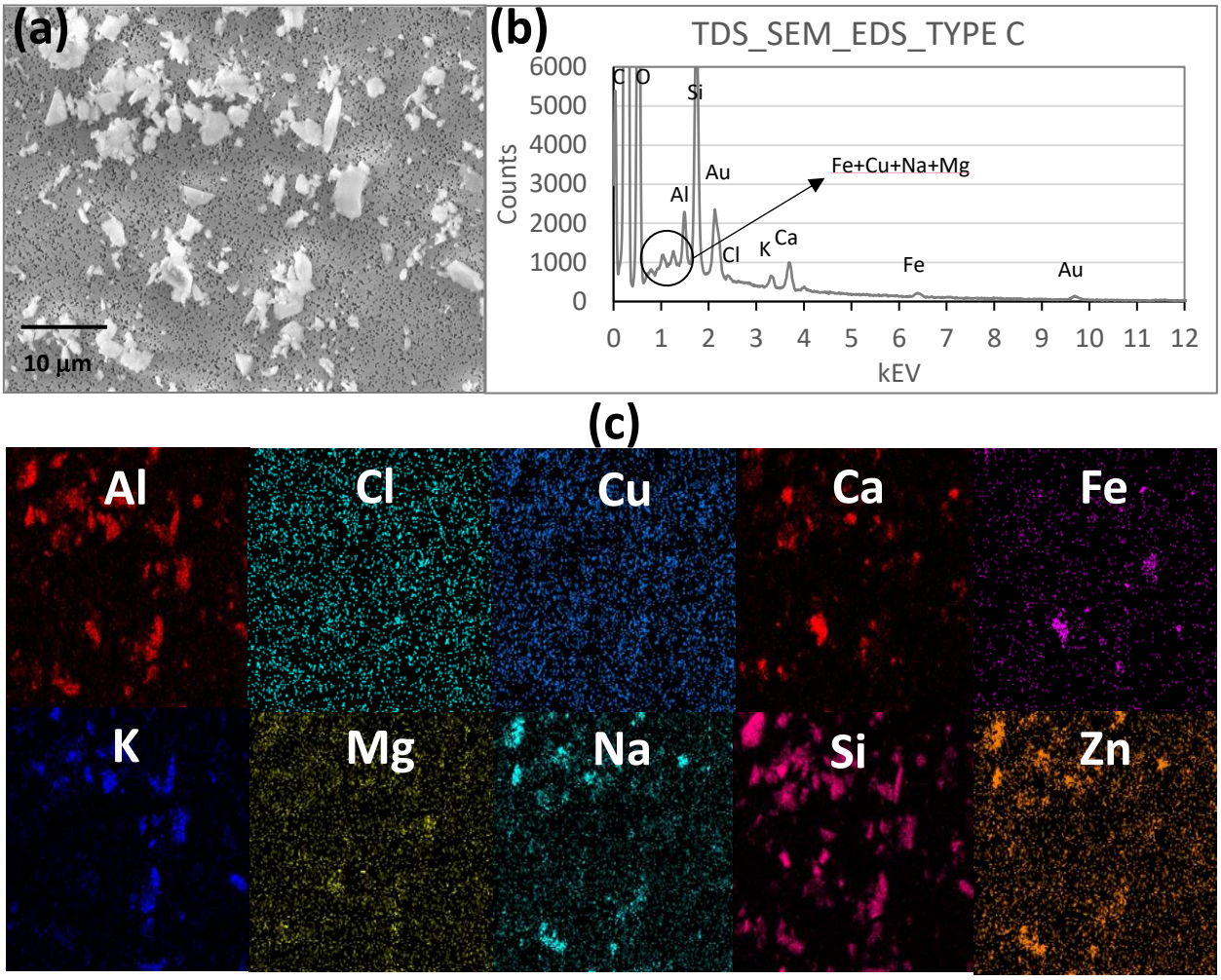

Figure S8. SEM and EDS analysis results of the image from product C by TDS. (a) Area selected for analysis. (b) Peaks analyzed by EDS. (c) Colorimetric elemental intensity analysis via EDS of a particle in image (a).

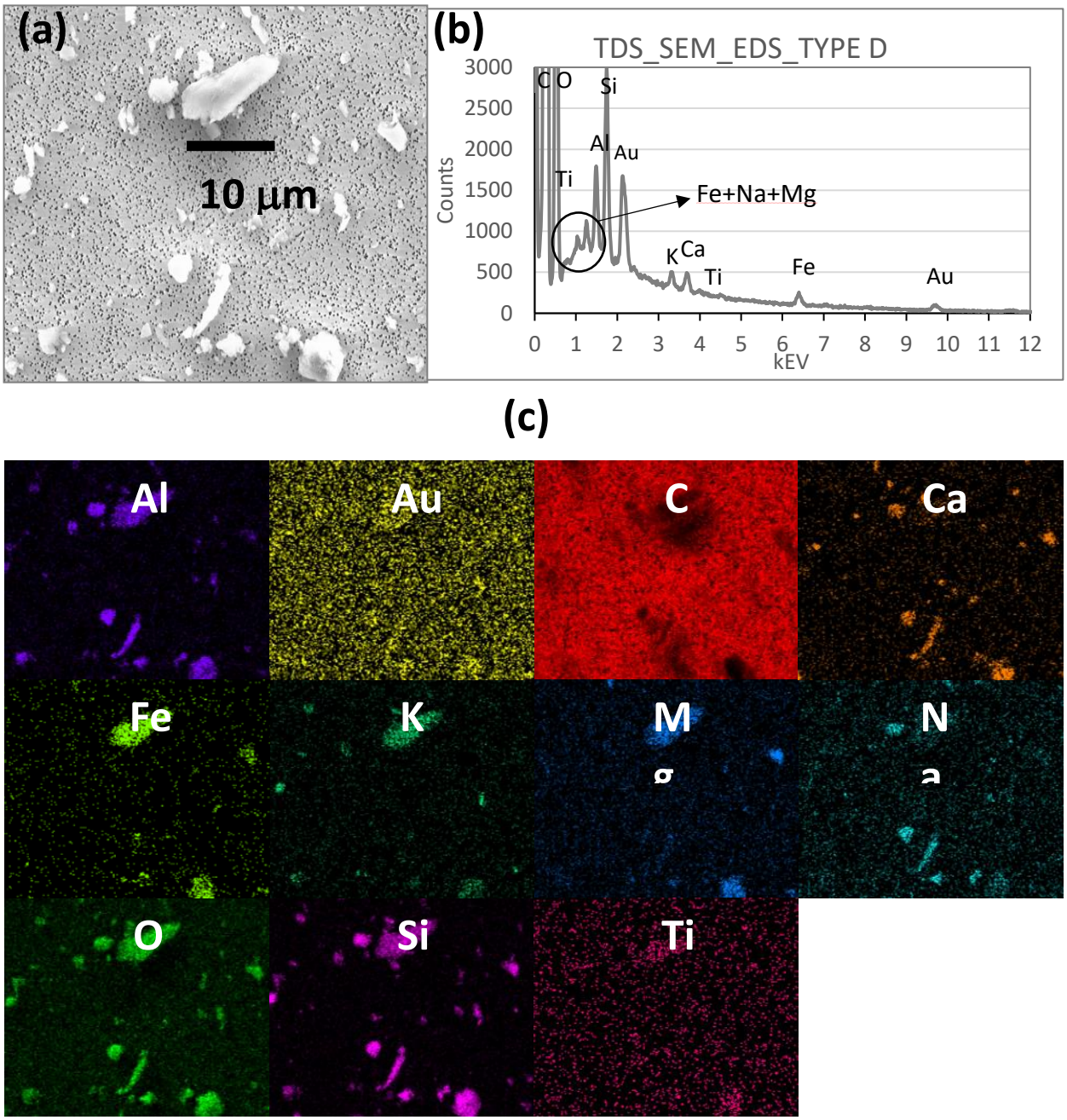

Figure S9. SEM and EDS analysis results of the image from product D by TDS. (a) Area selected for analysis. (b) Peaks analyzed by EDS. (c) Colorimetric elemental intensity analysis via EDS of a particle in image (a).

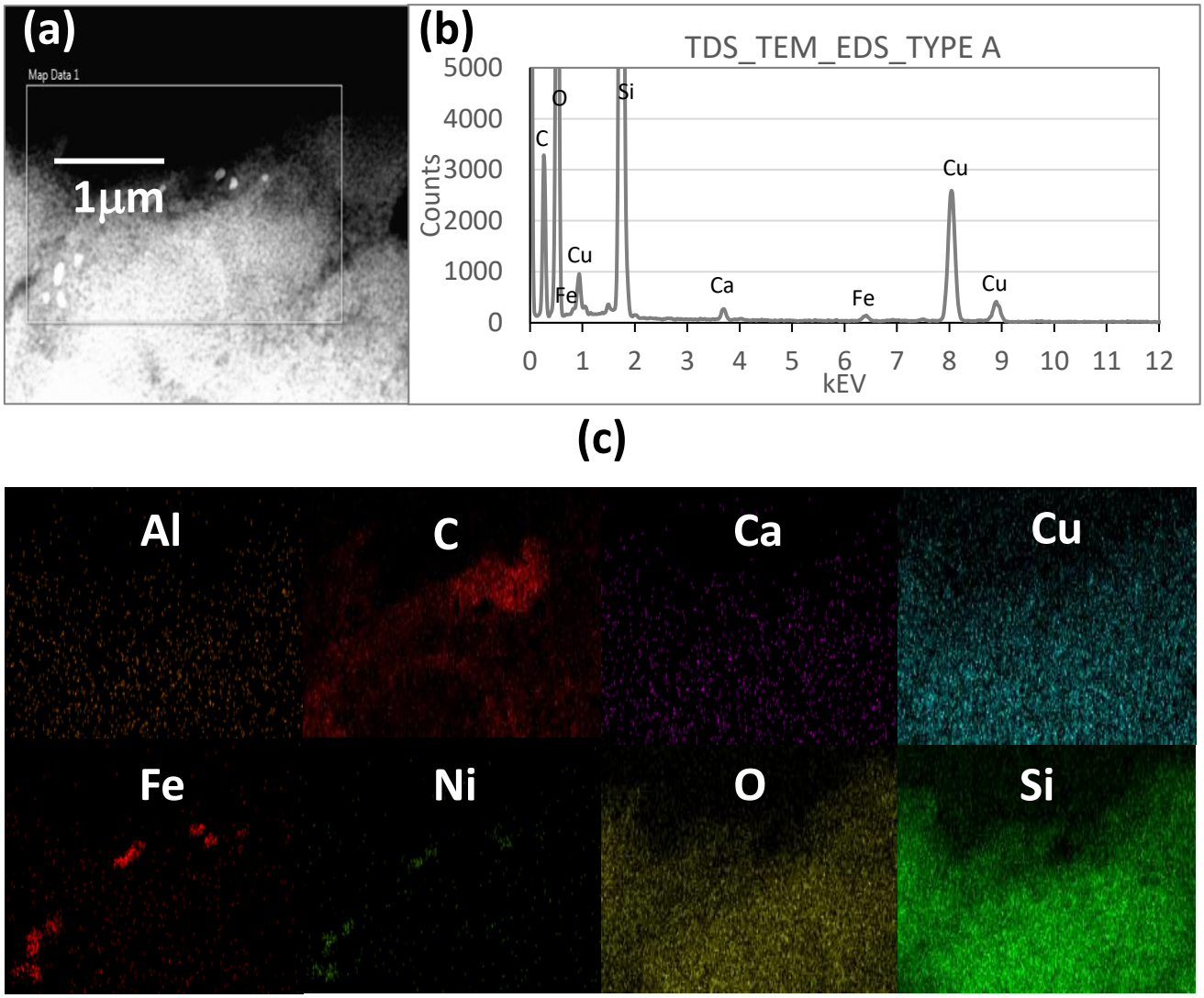

Figure S10. TEM and EDS analysis of particles collected from product A on a TEM grid by TDS. (a) The area of particles with small particulates attached to the edge,(b) Element peaks observed from analyzing the area in (a). (c) Colorimetric elemental intensity analysis via EDS for the area in (a).

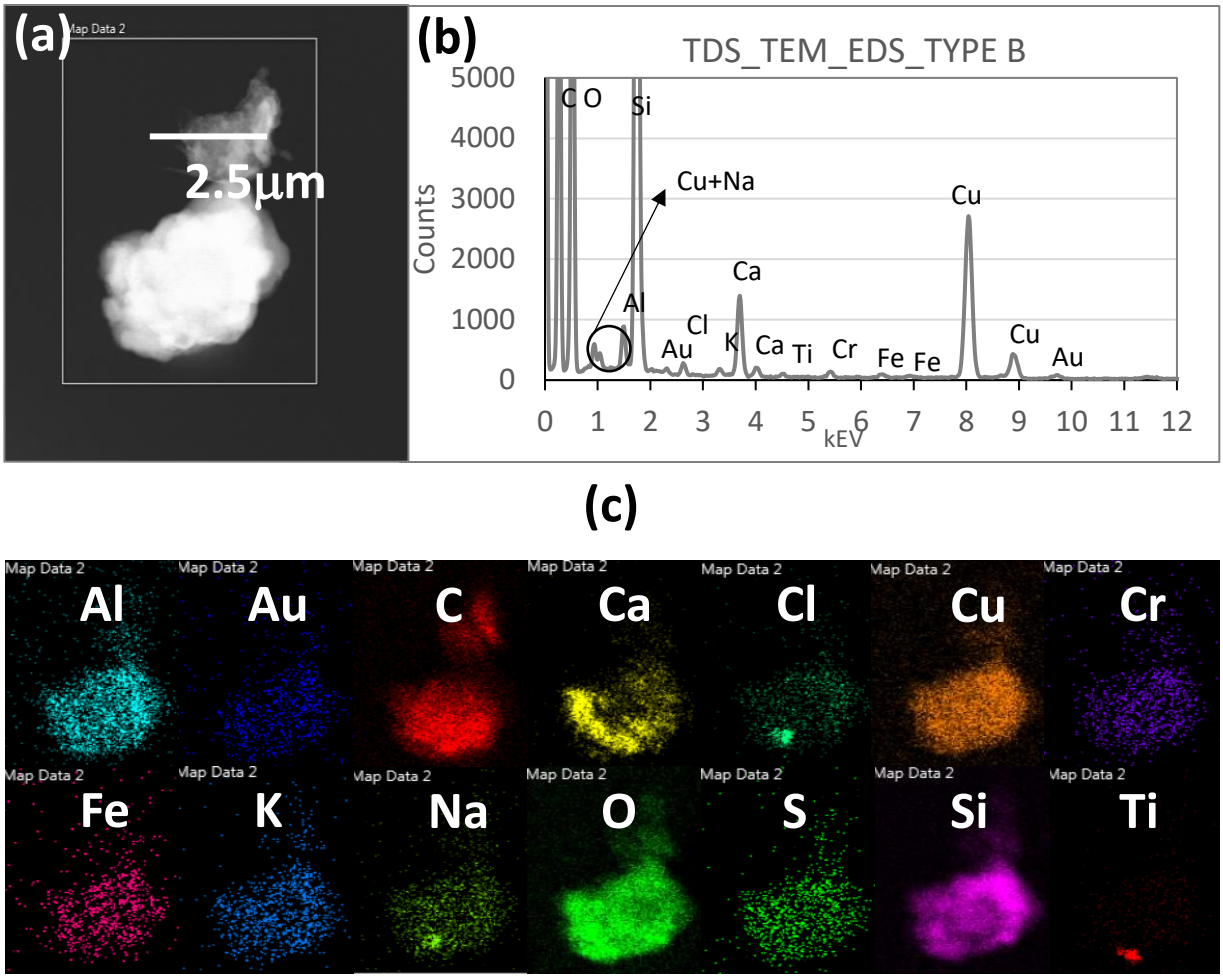

Figure S11. TEM and EDS analysis of particles collected from product B on a TEM grid by TDS. (a) The particle selected for EDS analysis, (b) Element peaks observed from analyzing the area in (a). (c) Colorimetric elemental intensity analysis via EDS for the area in (a).

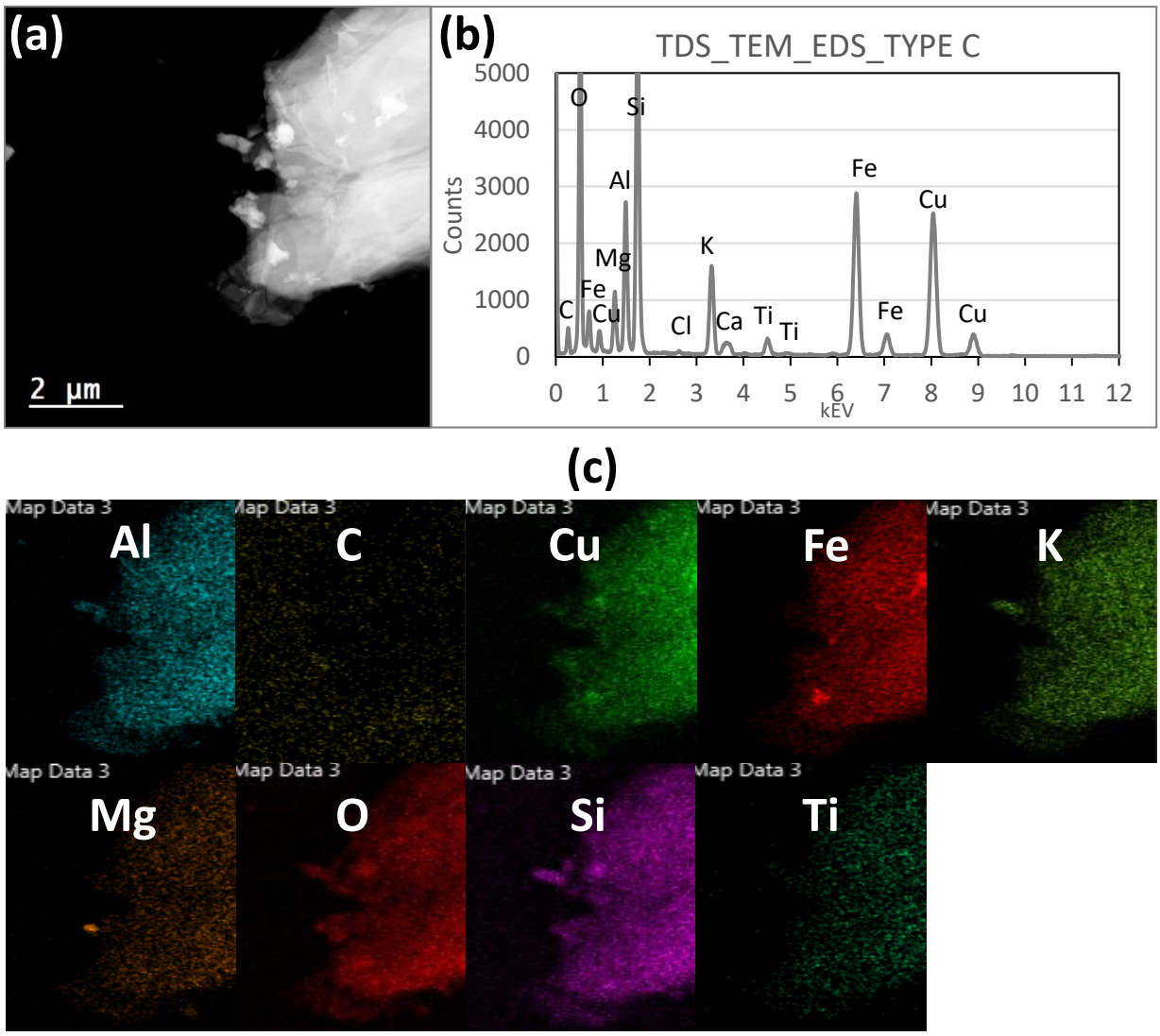

Figure S12. TEM and EDS analysis of the particles collected from product C on a TEM grid by TDS. (a) The area selected for analysis. (b) Element peaks analyzed by EDS. (c) Colorimetric elemental intensity analysis via EDS of image (a).

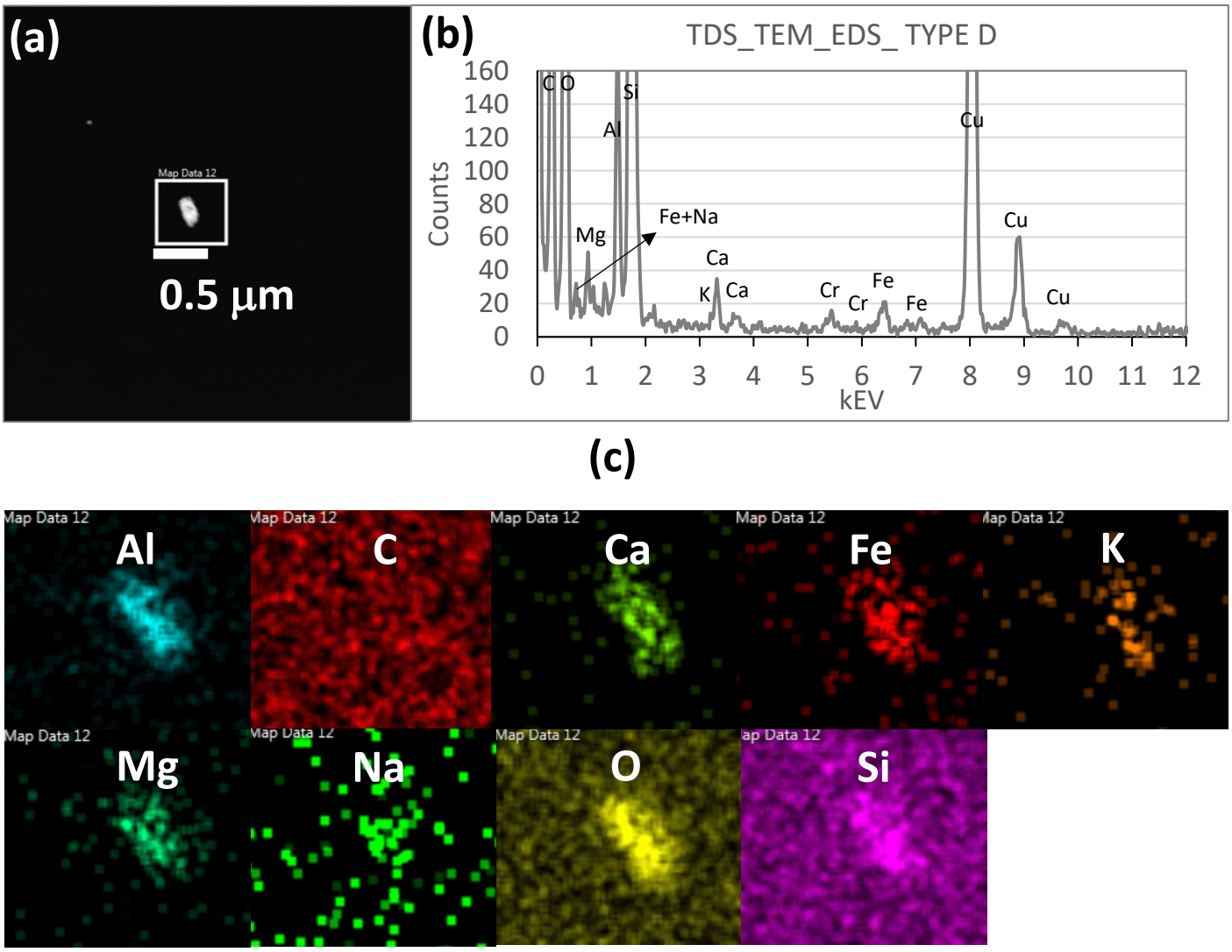

Figure S13. TEM and EDS analysis of the particles collected from product D on a TEM grid by TDS. (a) The area selected for analysis. (b) Element peaks analyzed by EDS. (c) Colorimetric elemental intensity analysis via EDS of image (a).

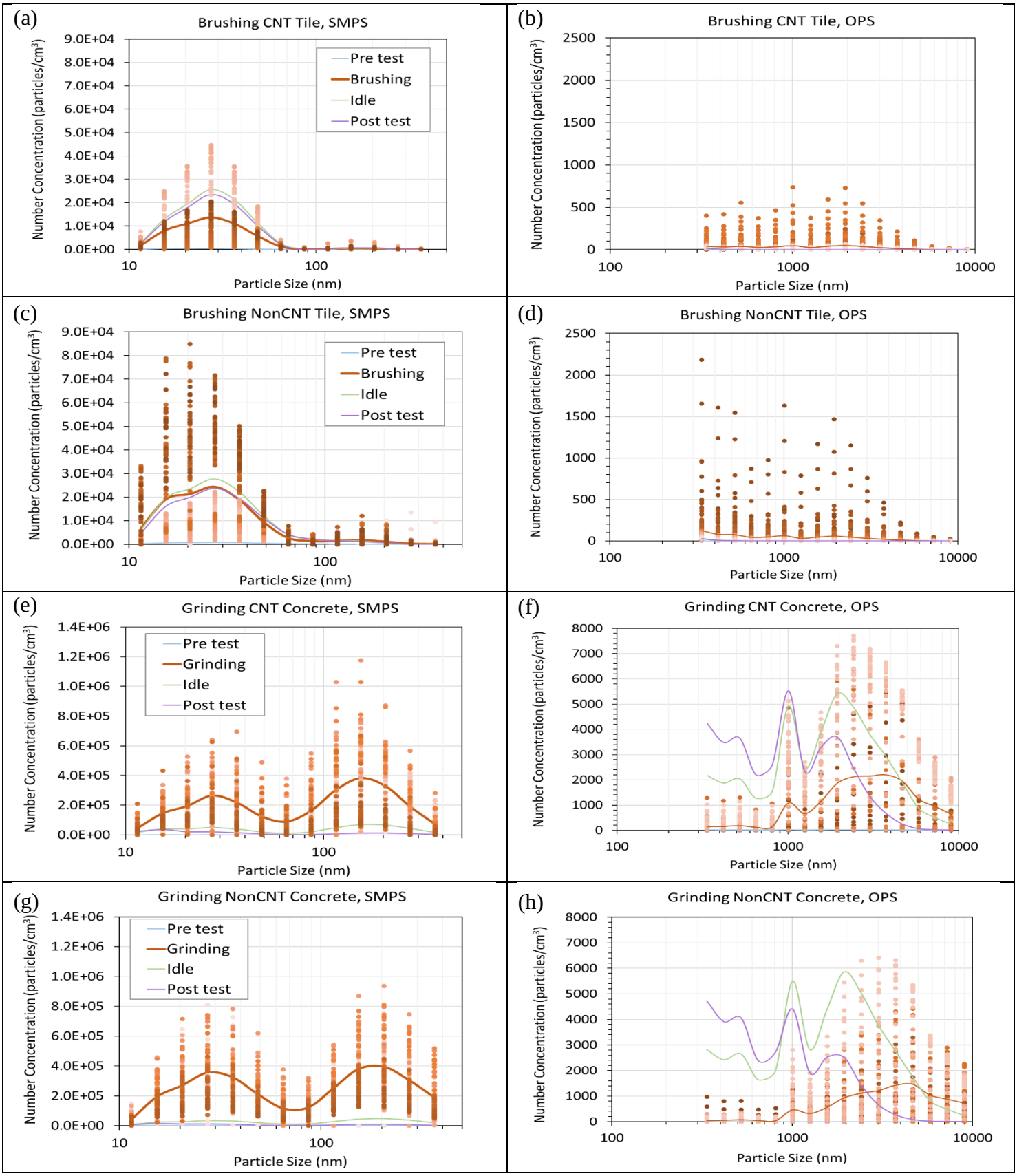
(a)
Brushing CNT Tile, SMPS
Number Concentration (particles/cm³)
Particle Size (nm)
Pre test
Brushing
Idle
Post test
(b)
Brushing CNT Tile, OPS
Number Concentration (particles/cm³)
Particle Size (nm)
(c)
Brushing NonCNT Tile, SMPS
Number Concentration (particles/cm³)
Particle Size (nm)
Pre test
Brushing
Idle
Post test
(d)
Brushing NonCNT Tile, OPS
Number Concentration (particles/cm³)
Particle Size (nm)
(e)
Grinding CNT Concrete, SMPS
Number Concentration (particles/cm³)
Particle Size (nm)
Pre test
Grinding
Idle
Post test
(f)
Grinding CNT Concrete, OPS
Number Concentration (particles/cm³)
Particle Size (nm)
(g)
Grinding NonCNT Concrete, SMPS
Number Concentration (particles/cm³)
Particle Size (nm)
Pre test
Grinding
Idle
Post test
(h)
Grinding NonCNT Concrete, OPS
Number Concentration (particles/cm³)
Particle Size (nm)

Figure S14. Particle size-fractioned concentrations in average with original concentration data during brushing shown in tan color dots. Concentrations in size range of 10-420 nm measured by NanoScan SMPS were shown on the left column. Concentrations in size range of 0.3-10 μm measured by OPS were shown on the right column. Concentrations were presented with measurements prior the test, during the testing activity (brushing or grinding), during idle period, and post the test. (a) and (b) Tests for brushing CNT coated tile, sample code A, (c) and (d) Tests for brushing non-CNT coated tile, sample code B, (e) and (f) Tests for grinding CNT containing concrete, sample code C, (g) and (h) Tests for grinding non-CNT containing concrete, sample code D.

Dynamic Aerosol Behavior

In the scenario of grinding concrete cylinder, we have seen that the sub-micrometer sized particles were the primary sizes of particles generated from the grinding activity according to the pattern of concentration changes. A similar aerosol dynamic also occurred under this grinding activity. However, in this scenario, although both sub-micrometer and micrometer sizes of particles generated from the grinding showed concentration changes following the grinding cycle, a more intense change was on the sub-micrometer sizes. The high amount of increases in the micrometer sizes (OPS measurement, Figures 4c and 4d) after the grinding has ended were mostly contributed by the agglomeration of small particles. Such particle agglomerations in the larger sizes than those seen in the brushing activity was also related to the orders higher of concentration in the small particles from the grinding activity.